

BRL R 1383

# BRL

AD

REPORT NO. 1383

## VAPORIZATION WAVES IN METALS

by

Frederick D. Bennett  
George D. Kahl

November 1967

D.D.C.  
RECEIVED  
FEB 16 1968  
A

This document has been approved for public release and sale;  
its distribution is unlimited.

U. S. ARMY MATERIEL COMMAND  
**BALLISTIC RESEARCH LABORATORIES**  
ABERDEEN PROVING GROUND, MARYLAND

AD 665369

BALLISTIC RESEARCH LABORATORIES

REPORT NO. 1383

NOVEMBER 1967

VAPORIZATION WAVES IN METALS

Frederick D. Bennett  
George D. Kahl

Exterior Ballistics Laboratory

This document has been approved for public release and sale;  
its distribution is unlimited.

RDT&E Project No. 1T014501A33D

ABERDEEN PROVING GROUND, MARYLAND

BALLISTIC RESEARCH LABORATORIES

REPORT NO. 1383

FDBennett/GDKahl/sjw  
Aberdeen Proving Ground, Md.  
November 1967

VAPORIZATION WAVES IN METALS

ABSTRACT

The vaporization wave hypothesis is discussed and its merits and defects are examined. The vaporizing model is visualized on thermodynamic grounds as carrying the liquid metal through a continuous succession of states either on or near the liquidus line in the two-phase region. On this line the adiabatic sound speed for wet vapor will limit the rate of propagation of the vaporization front into the liquid. Experimental data for wire explosions of Al, Ag, Cu, Au, Pb and Hg (frozen) are analyzed for wave speeds. While the influence of thermal expansion of the liquid can be accounted for theoretically, insufficient thermal data are available for the metals to permit correction of the wave speeds for this effect. The experimentally derived wave speeds are compared with theoretical values of the adiabatic sound speed in the wet vapor obtained from a modified, van der Waals equation of state. At low velocities the agreement is satisfactory but higher values deviate considerably from theory.

Possible causes of the deviations are discussed. These include the crudity of the fluid dynamic model, neglect of thermal expansion, lack of information about the relationship between density and electrical conductivity and the approximation imposed by the van der Waals equation.

TABLE OF CONTENTS

|                                 | Page |
|---------------------------------|------|
| ABSTRACT . . . . .              | 3    |
| INTRODUCTION . . . . .          | 7    |
| THERMODYNAMICAL MODEL . . . . . | 12   |
| EXPERIMENTAL . . . . .          | 20   |
| DISCUSSION . . . . .            | 39   |
| SUMMARY . . . . .               | 45   |
| REFERENCES . . . . .            | 47   |
| DISTRIBUTION LIST . . . . .     | 49   |

## INTRODUCTION

We discuss here some recent experiments to examine further the hypothesis that vaporization waves are responsible for the anomalous resistance rise in exploding wires. While vaporization waves may be expected in all high temperature matter on general thermodynamic grounds,<sup>1,5\*</sup> the first instance in which their existence could be recognized appears to be the exploding wire phenomenon.<sup>2</sup> If the vaporization of a superheated metal cylinder is limited by the speed with which the head of the vaporization wave travels from periphery to the axis, then an upper bound is set on the rate at which the conducting cross section diminishes. Resistance increases above the melting point, larger than the usual linear rise with temperature, can be related to the decreasing cross section of the conductor; thus, wave speeds can be obtained from the electrical pulse data. In our earlier paper<sup>2</sup> we reported wave speeds for Cu wires. Here we present data for Cu, Pb, Al, Au, Ag and Hg (frozen) wires and make comparison with predictions from theory.

From a critic's point of view a number of limitations on the applicability of the vaporization wave hypothesis can be stated.

The success of the experimental method of analysis depends on the assumption of a linear relation between resistivity and specific energy applied above the melting point up through the two-phase region. This is, at best, a fairly crude approximation but cannot be replaced until better information is available. Certain metals such as Fe, Ni and W

---

\*Superscript numbers denote references which may be found on page 47.

display nonlinear resistivity decreases above the melting point; and, therefore, cannot be treated by the present method. In the case of W, at least, we know now that these nonlinear effects are associated with conduction and arc phenomena in the peripheral vapor emitted by the wire during expansion. There is reason to hope that eventually wave phenomena may be studied in W wires immersed in a dielectric liquid such as silicone vacuum pump oil. Needless to say, the effects of a dense ambient medium on the wave propagation and the electrical pulse shape are not well understood, although some preliminary unpublished experiments show that voltage breakdown and peripheral arc formation can be slightly delayed by ambient liquids of high breakdown strength.

At the relatively high densities of the exploding wire experiment, collision frequencies are high ( $\sim 10^{15}$ /sec), the liquid and vapor should obey continuum fluid mechanics, and local thermodynamic equilibrium may be assumed from point to point in the medium.

To discuss the fluid dynamical behavior of a superheated metal, one desires to specify a homogeneous, high temperature medium at uniform pressure as the initial state. For the fast explosions in which we are interested a plausible argument can be given that nearly uniform conditions exist, at least for the early phases of the explosion. This means assuming that transient skin effect has damped out, that kinetic pressures rapidly exceed magnetic pinch pressures and that heat losses via conduction, convection and radiation can be neglected on the time

scale of the experiment. Estimates based on simplified calculations of the expected effects show that these conditions may be satisfied for events occurring within intervals of a few  $\mu\text{sec}$ .

Dynamical effects themselves may be expected to lead to non-uniformities of pressure, temperature and density throughout the medium as the flow develops. Figs. 1 and 1a show that density variations occur rather early in the expansion process. What, then, is the initial state and how uniform is the expansion which follows?

X-ray and optical shadowgraphs have already shown that the later stages of the expansion proceed with large density differences between adjacent portions of the wire. Apparently vapor and dense striations exist side by side during appreciable intervals of the expansion process. Formerly we supposed that these nonuniform densities occurred late in the expansion regime, after the vaporization wave had traversed the wire radius. Fansler and Shear<sup>4</sup> demonstrate by means of x-ray shadowgraphs, correlated in time with electrical pulse data, that striations appear at a much earlier stage than previously thought, and must be regarded as practically concurrent with more elementary expansion processes such as volume expansion of the liquid in the two-phase region and expansion through the head of the vaporization wave.

Light scattering studies of the metal vapor peripheral to the wire, studies made at this laboratory and to appear soon in report form, indicate appreciable particle-size changes during the expansion process.

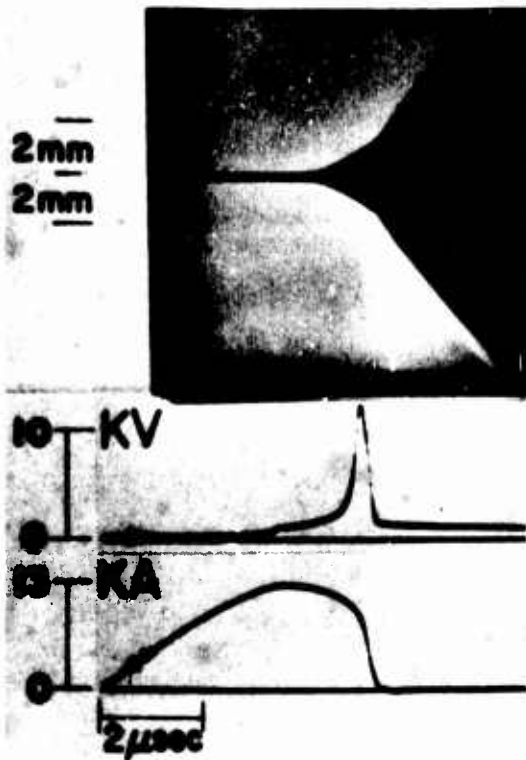


Figure 1. Correlated electrical and streak camera data for 10 mil Cu wire. ( $V = 3 \text{ kV}$ ,  $C = 32 \text{ } \mu\text{F}$ )



Figure 1a. Enlargement of expansion region of Figure 1. Note that the vapor veil is penetrated by the backlighting. Luminosity from the interior is seen just after voltage peak

In the light of these experimental indications we recognize that the ideal of a homogeneous medium expanding from uniform initial conditions continues to be elusive.

The presence of visible density striations in the early expansion stages would militate against the assumption of a uniform vaporization wave diminishing the conducting cross section at a definite, though variable speed. Rather one may ask what conduction processes could simultaneously involve the striations and the nearby less dense regions. One may also ask whether the striations arise from nonuniformities of heating or from initial conditions in the crystalline solid wire, or whether striations form because of local condensation from a more uniform, vaporous state attained soon after melt and prior to the violent expansion.

No matter what the answers to these questions, the viability of the vaporization wave hypothesis, at least in its application to exploding wires, is clearly still open to question; nevertheless, one cannot say that it is decisively disproven by experiment.

The evidence in its favor is compelling. Our results show that experimentally derived wave speeds correlate with those calculated from a van der Waals equation of state for metals. Both the onset energy and the form of the wave speed function are correctly represented. In terms of scaling laws based on critical temperatures, the wave speed curves for several metals cluster about the single theoretical curve. These results provide an independent check of recent

methods of estimating critical temperatures hitherto inaccessible to measurement. One cannot readily reject a theoretical approach with demonstrable virtues such as these. One hopes that by refinement its deficiencies can be eliminated; however, the loss of its initial fine simplicity is to be expected in the ensuing complications.

#### THERMODYNAMICAL MODEL

In this section, a simplified fluid model will be developed to represent the transient behavior of a material heated rapidly from the solid state up through its critical temperature. For typical metals, the heat energy for melting is small compared to that required to vaporize the system; therefore, we concentrate on the mechanism of the liquid-vapor transition. For such a two-phase condensing fluid, there are a variety of state equations. The most famous is van der Waals equation, which typifies the essential features of a condensing fluid, and which will herein be used in a slightly modified form.

Consider unit mass of material, and let  $P$ ,  $V$ , and  $T$  be pressure, specific-volume and temperature, respectively. In the single phase (either liquid or vapor) the pressure is assumed given by the van der Waals function,  $P_w$ ,

$$P_w(V,T) = \hat{R}T/(V-b) - a/V^2, \quad (1)$$

with inequalities  $T > 0$ ,  $V \geq b$ , where  $\underline{a}$  and  $\underline{b}$  are substantive

constants for each material and  $\hat{R}$  is the gas constant. For subcritical temperatures there is a two-phase region where both the liquid and vapor phases coexist at the same pressure and temperature; in coexistence, the pressure is not that given by Eq. (1) above; instead it is the vapor pressure function  $P_A(T)$ . For the van der Waals system, this latter function is not explicitly represented by an analytic function and must be found by computation. To compute  $P_A(T)$  as well as the  $V_3(T)$  and  $V_1(T)$  loci of the saturated liquid and vapor lines, a generalization of the Maxwell criterion<sup>5</sup> is used, so that at fixed  $T < T_c$  (subscript  $c$  always denotes critical conditions),

$$\int_{V_3(T)}^{V_1(T)} P_w dV = P_A(T) \{V_1(T) - V_3(T)\} + \phi(T) \quad (2)$$

where

$$\phi(T) = \int_{T_c}^T -\{C_v(\tau)(\text{vapor}) - C_v(\tau)(\text{liq})\} d\tau + T \int_T^{T_c} \{C_v(\tau)(\text{vapor}) - C_v(\tau)(\text{liq})\} \frac{d\tau}{\tau} \quad (3)$$

Here  $C_v$  is the specific heat at constant volume of the single phases. For either phase,  $C_v(T)$  is a function of temperature only, and is chosen to be consistent with the van der Waals system. If  $C_v(T)$  (vapor) is identical with  $C_v(T)$  (liq) then  $\phi(T)$  is zero and (2) reduces to the usual "equal area" rule first given by Maxwell. We note that the

equal-area rule is restrictive in demanding identical specific heat functions for the liquid and vapor phases. This restriction is lifted when the generalized rule above is used, but its use requires some information about specific heats. The constants  $\underline{a}$  and  $\underline{b}$  for the material are conveniently replaced in terms of the critical values of the system by the well-known relations:

$$\underline{a} = 3 P_c V_c^2 ; \underline{b} = V_c/3 ; \hat{R} T_c = (8/3) P_c V_c . \quad (4)$$

Knowledge of the critical constants as well as of the specific heats completes the description of the equilibrium state of the system. One can now find all the pertinent thermodynamical quantities, including those of the coexistence state. These will be explicitly exhibited as needed.

We use this model to analyze the behavior of materials heated from comparatively low temperatures. In particular, we consider a system in the molten state just above the melting temperature, and allow it to be heated to critical conditions. The usual adiabatic speed of small amplitude waves (sound speed) in the system is given by  $c^2 = (dp/d\rho)_{ad}$  which becomes, with  $\rho = 1/V$ ,

$$c^2 = - V^2 \left( \frac{dP}{dV} \right)_{adiabatic} = V^2 \left\{ \frac{T}{C_v} \left( \frac{\partial P}{\partial T} \right)_V^2 - \left( \frac{\partial P}{\partial V} \right)_T \right\} . \quad (5)$$

For the condensing fluid, we note that the pressure and specific heat functions are different for the single phase regime and for the two-phase coexistence state. In the single phase regime, we use the van der Waals functions, whereas in coexistence we use the vapor pressure function,  $P_A(T)$ , and the specific heat  $C_{VA}(V,T)$  of coexistence. Since  $P_A$  is independent of volume, the wave speed in coexistence reduces to  $c_w$ , where

$$c_w = V(T/C_{VA})^{1/2} \left( \frac{dP_A}{dT} \right) . \quad (6)$$

At the saturated liquid line, there are two very different values of wave speed possible; which one applies depends on whether the disturbing wave tends to change the system to the single phase (all liquid) state, or to the two-phase state.

The specific heat  $C_{VA}(V,T)$  for the coexistence state must also be found numerically. This is done straightforwardly by finding the internal energy,  $E_A$ , of coexistence, and using  $C_{VA} = \left( \frac{dE_A}{dT} \right)_V$ . The internal energy of coexistence is found by using  $E_A$  and  $P_A$  for  $E$  and  $P$  in the general thermodynamical relation

$$\left( \frac{\partial E}{\partial V} \right)_T = T \left( \frac{\partial P}{\partial T} \right)_V - P \quad (7)$$

and noting from Eq. (2) that  $M(T) = T \frac{\partial P_A}{\partial T} - P_A$  is independent of  $V$  ;

then direct integration yields

$$E_A(V,T) = E_M(V_3,T) + M(T) \{V - V_3(T)\} , \quad (8)$$

where  $E_M$  is the internal energy of the van der Waals function. One then finds

$$C_{VA}(V,T) = \left[ \frac{dE_M(V_3,T)}{dT} \right] + \frac{dM(T)}{dT} \{V - V_3(T)\} - M(T) \frac{dV_3(T)}{dT} , \quad (9)$$

noting that

$$\left[ \frac{dE_M(V_3,T)}{dT} \right] = \frac{\partial E_M}{\partial V_3} \frac{dV_3(T)}{dT} + \frac{\partial E_M}{\partial T} . \quad (10)$$

For example, at the saturated liquid line, the specific heat of co-existence simplifies to

$$C_{VA}(V_3,T) = \left\{ \frac{\partial E_M}{\partial V_3} - M(T) \right\} \frac{dV_3(T)}{dT} + \frac{\partial E_M}{\partial T} . \quad (11)$$

The last term on the right is the constant-volume specific heat of the

liquid;  $\frac{\partial E_M}{\partial V_3} = a/V_3^2$ , as may be seen by using  $E_M$  and  $P_M$  in Eq. (7).

With  $P_A(T)$  and  $V_3(T)$  found from Eqns. (2) and (3) we may now evaluate the two possible wave speeds on  $V_3(T)$ . These are exhibited in non-dimensional form in Fig. 2 as functions of  $T/T_c$  for the example where  $C_v(\text{liq}) = C_v(\text{vap}) = (3/2) \hat{R}$ .

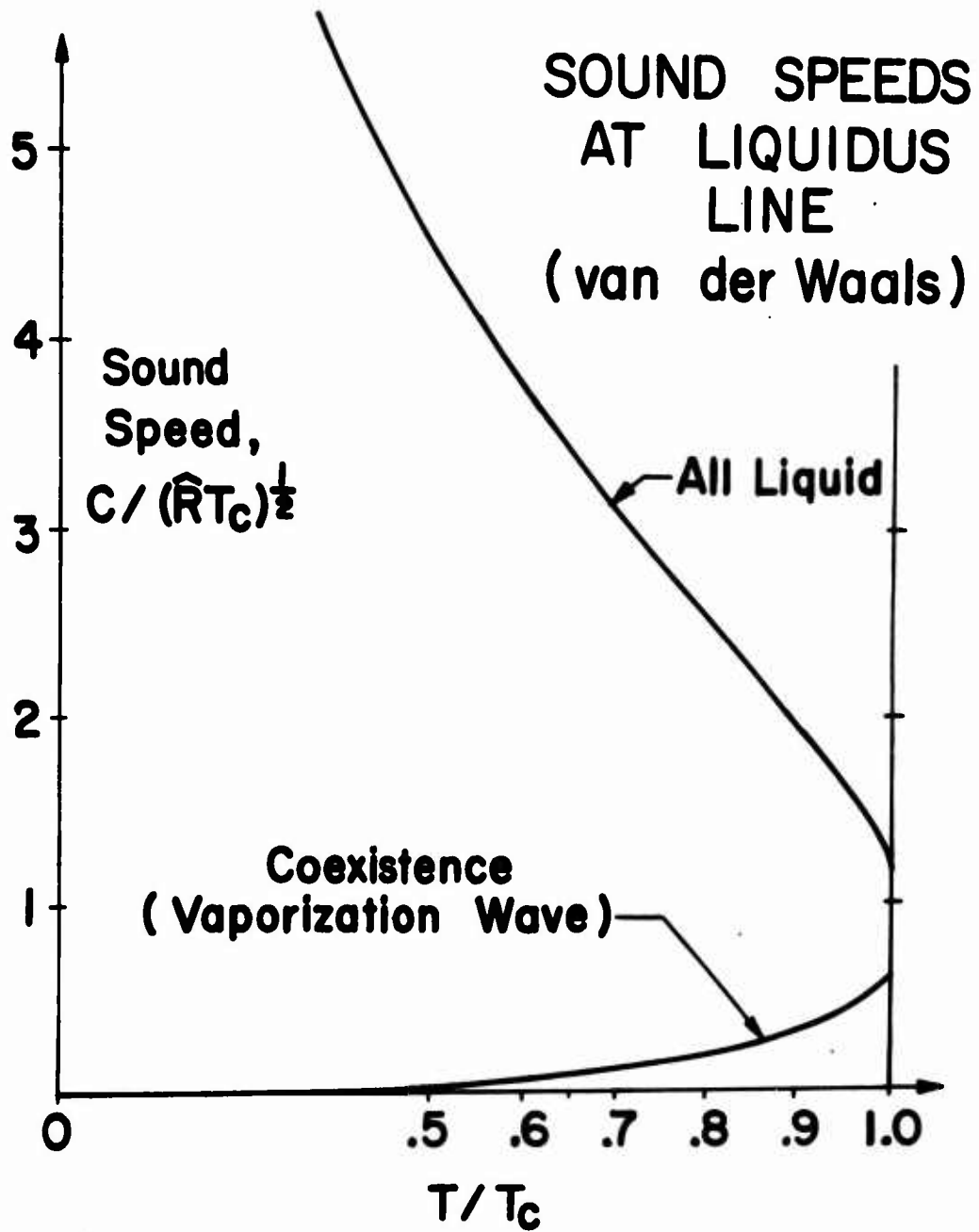


Figure 2. Double valued sound speeds on liquidus, van der Waals-Maxwell fluid,  $[C_V(\text{liq}) = C_V(\text{vap}) = (3/2)R]$

The wave speed in the liquid is seen from Fig. 2 to be very much larger than the vaporizing wave speed of the two-phase system. The vaporizing wave speed is very small until temperatures exceeding one-half critical are attained.

It is characteristic of the van der Waals system (and indeed of most physical examples) that both the isotherms and adiabatics in the all-liquid phase are very steep compared to those of either the co-existence or all-vapor states, except very near the critical point. The magnitudes of these adiabatic slopes are directly proportional to the squared sound speed, so one expects the liquid sound speed to be usually much higher than the vapor or vaporizing wave speeds.

This fact suggests a simplification of our model for the system undergoing transient heating from an initially molten state at low temperatures. We assume that the heating moves the thermodynamic state along the saturated liquid line; any tendency to drive the system into the all-liquid state would be rapidly counteracted by liquid thermal expansion, which occurs at a relatively fast rate corresponding to liquid sound speed. This liquid thermal expansion lowers the pressure to the vapor pressure,  $P_A(T)$ , where any further expansion must be accompanied by partial vaporization. This latter expansion is governed by the relatively slow vaporizing wave speed of the coexistence state. We note that due to the steepness of the all-liquid adiabatics, only a small volume increase is needed to maintain the system at the saturated liquid state.

We therefore assume the fluid state of the exploding wire in the pre-burst stage can be approximated by a molten cylinder from whose surface partial vaporization is occurring. The speed of the leading edge of this partially vaporizing wave is assumed to move with the vaporizing sound speed of the saturated liquid at temperature  $T$ , and is given by Eq. (6).

It is of interest to correlate the vaporizing wave speed with the added heat content,  $q$ , per unit mass, rather than temperature, because the additional heat energy can usually be found operationally by energy balance, whereas temperature is a more elusive quantity. In particular, for the modified van der Waals system employed here, one can compute the equilibrium heat content per unit mass along the saturated liquid line by using Eq. (2), and the assumed known critical constants and liquid specific heat. One integrates

$$dq = dE + PdV \tag{12}$$

along the saturated liquid line,  $V_3(T)$ , from  $T_m$  to  $T$ , where  $T_m$  is melting temperature, using computed values of  $E_w(V_3, T)$  and  $P_A(T)$  from Eqns. (2) and (3). At any  $T$  between  $T_m$  and  $T_c$ , a quantity  $\Delta q(T)$  is obtained, thus giving a correspondence between  $\Delta q(T)$  and  $T$ . For a given material, one then assumes the heat content along the saturated liquid line to be

$$q(T) = q(T_m) + \Delta q(T), \quad (13)$$

where  $q(T_m)$  is the assumed known heat content of the liquid at melt, including the latent heat of melting. It is apparent that  $q(T)/\hat{RT}_c$  depends on the specific heats of the liquid and vapor phases through Eqns. (1) and (2), as well as on  $q(T_m)/\hat{RT}_c$ . This latter quantity is found to have nearly the constant value of .60 for a variety of metals, so plots of  $c_w/(\hat{RT}_c)^{\frac{1}{2}}$  against  $q/(\hat{RT}_c)$ , where  $c_w$  is the vaporizing wave speed or  $V_s(T)$ , usually depend only on the single-phase specific heats as parameters. We exhibit such plots in Fig. 3 for several examples of specific heats.

#### EXPERIMENTAL

We outline here the procedure for calculating vaporization wave speeds from the electrical data. This method differs somewhat from that given previously,<sup>2</sup> in that a means of accounting for thermal expansion of the liquid metal is incorporated in the present scheme.

##### Data Reduction for Wave Speed

The voltage across the wire and the current through it are obtained from oscilloscope traces as previously described.<sup>6</sup> After accounting for the inductive voltage on the voltage probe, one then has the resistive voltage,  $V_r$ , as a function of time. Typical  $V_r(t)$  and  $I(t)$  measurements are seen in Fig. 1. We assume the rapid increase

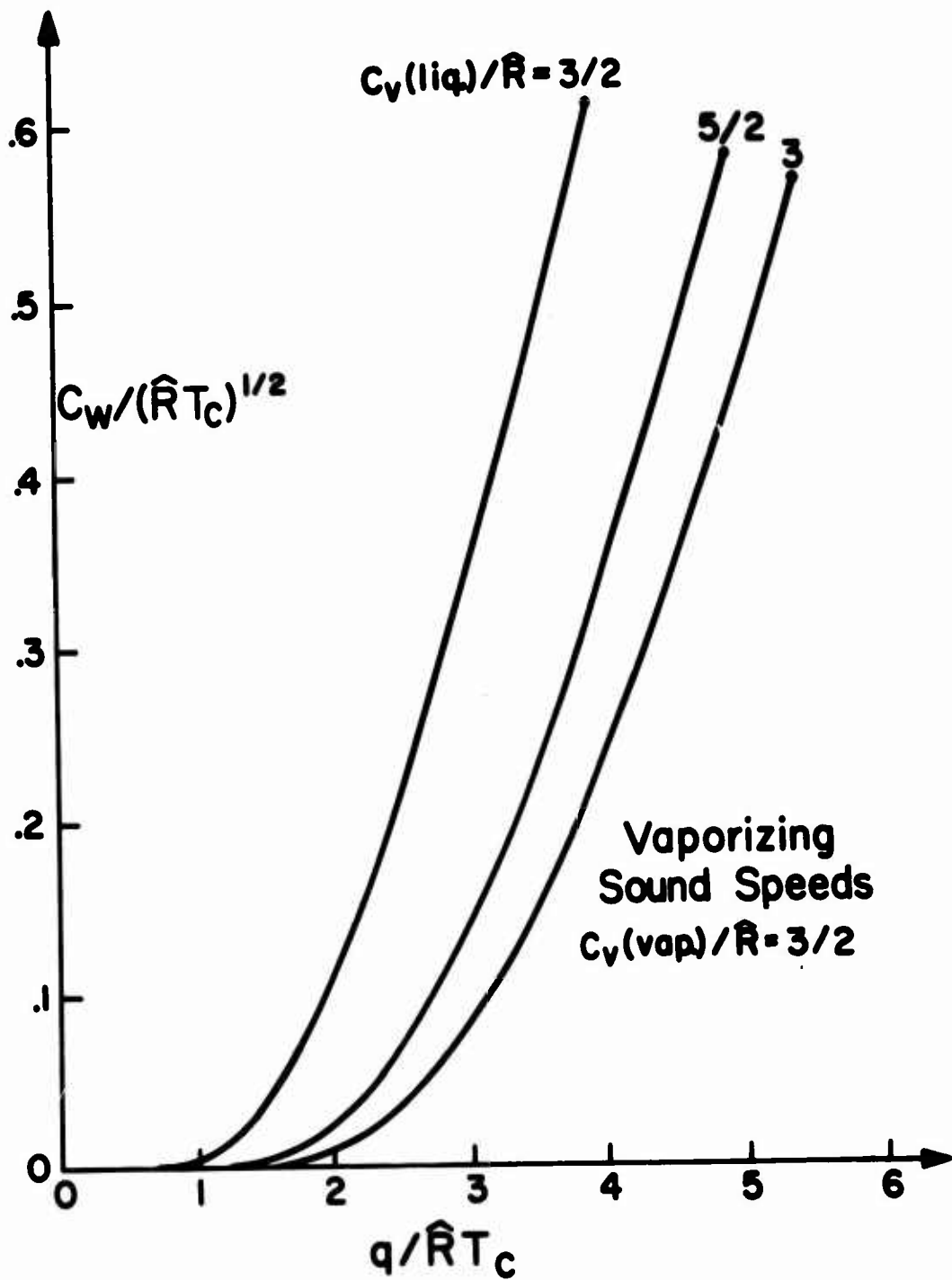


Figure 3. Vaporizing sound speed on liquidus. A modified van der Waals equation has been used with liquid specific heat as a parameter. Curves terminate at the heat energy of the critical point

of voltage to its peak is due to an increasing resistance caused primarily by a reduction of the conducting cross section of the molten wire; this reduced cross section is attributed to the partial vaporization proceeding inward from the wire surface.

#### Pre-Vaporization Heating of the Liquid Metal

As heat is added to the molten metal a slight thermal expansion will occur. Since the length-to-radius ratio of the wire is large, expansion waves traveling at the local speed of sound will not reach the wire ends during the short time interval of the explosion. We therefore expect the thermal expansion to be effective in increasing the radial dimension only, and account for it by assuming the entire mass is contained within a cylinder of length of that of the original wire,  $l$ , and average radius  $r_1(t)$ . It is clear that  $r_1(t)$  must increase slightly with time, according to the heat addition and consequent average density decrease of the liquid.

In order to describe the assumed model of the wire explosion, we wish to map certain boundary, wave path, and particle trajectories in an  $r, t$  plane. If  $m_s$  represents the mass of the solid wire and  $m$  the mass of the wire within radius  $r$  before vaporization, we can write  $m = \pi r^2 l d(t)$  where  $d(t)$  is the uniform density of the metal, a density which varies only with time. For  $m$  constant, it follows that  $r \equiv r(m, t)$  describes the variation with time, due to thermal expansion, of the representative mass particle at the radius which encloses mass  $m$ . In

this mapping  $m$  is a parameter and  $t$  the variable of interest. Accordingly,  $r_1(t) = r(m_s, t)$  gives the curve in the  $r, t$  plane of the expanding outer boundary of the liquid wire. Because of the assumption of uniform density all other particle trajectories corresponding to  $m \leq m_s$  are similar curves.

The trajectory of the vaporization wave, which we denote by  $r_2(t)$ , cuts across the particle trajectories in passing from larger to smaller radii. With the above definitions we could write  $r_2(t) = r[m_2(t), t]$  where  $m_2(t)$  represents the variable mass ahead of the vaporization wave at time  $t$ . Here the parameter  $m$  changes from point to point of the  $r_2$  curve; however,  $m_2$  is not known a priori but must be determined from experiment.

### Vaporization Model

With increased heat content of the liquid, the threshold of vaporization will be exceeded and a wave will start. We assume that the cylindrical interface of average radius  $r_2(t)$  separates the intact molten core from the outer, nonconducting, partially vaporized mixture. The local velocity of this interface in a reference frame fixed with a given set of fluid particles is denoted by  $c_r$ . In a laboratory fixed reference frame the interface velocity is

$\frac{dr_2(t)}{dt}$ . The velocity of the liquid particles at  $r = r_2(t)$  (which

is the same as the velocity of the reference frame attached to these

particles), is  $\left\{ \frac{dr}{dt} \right\}_{m_2}$ .

Therefore,

$$c_r = \left\{ \frac{dr(t)}{dt} \right\}_{m_2} - \frac{dr_2(t)}{dt} \quad (14)$$

If no vaporization occurred, the entire liquid mass,  $m_3$ , of the wire would be contained within the radius  $r_1(t)$ . Assuming the density of the liquid core to be constant with radius, the mass  $m$  ( $< m_3$ ) contained within  $r(t)$ , [ $r_2(t) \leq r_1(t)$ ], is related to the total mass by  $r(t) = (m/m_3)^{\frac{1}{2}} r_1(t)$ . Differentiating this expression, and noting that both  $m$  and  $m_3$  are time-independent, we find

$$\frac{dr(t)}{dt} = (m/m_3)^{\frac{1}{2}} \frac{dr_1(t)}{dt} \quad (15)$$

The mass,  $m_2(t)$ , of material contained within  $r_2(t)$  does change with time, since  $r_2(t) = (m_2/m_3)^{\frac{1}{2}} r_1(t)$ . With the foregoing relations

$$c_r = - r_1(t) \frac{d}{dt} \left\{ (m_2/m_3)^{\frac{1}{2}} \right\} \quad (16)$$

The electrical resistance,  $R_2$ , of the conducting cylinder of radius  $r_2(t)$  is

$$R_2/R_0 = \frac{\rho(t)}{\rho_0} \left[ \frac{r_0}{r_2(t)} \right]^2, \quad (17)$$

where subscript 0 denotes some suitably chosen reference conditions which identify the beginning of the wave, and  $\rho$  is the electrical resistivity. Furthermore, if  $d(t)$  be the liquid density of the core, we have

$$m_2(t)/m_3 = \left[ \frac{r_2(t)}{r_0} \right]^2 \frac{d(t)}{d_0}. \quad (18)$$

The rate at which total heat,  $Q$ , is added to the core is

$$\frac{dQ}{dt} = I(t) V_r(t) = I(t)^2 R_2(t), \text{ a measured quantity. Since this heat}$$

input is assumed to be deposited uniformly in the conducting cylinder by uniform current distribution we can write  $\frac{dQ}{dt} = m_2 \frac{dq}{dt}$ , where  $q$  is the heat content per unit mass. With the foregoing relations we then have

$$\left( R_2(t)/R_0 \right) \frac{dQ}{m_3} = \left\{ \left( \frac{\rho(t)}{\rho_0} \right) \frac{d(t)}{d_0} \right\} dq. \quad (19)$$

Using the experimental values of  $V_r(t)$  and  $I(t)$ , we can numerically integrate the left-hand side from the reference conditions  $R(Q_0)$  to

the values for  $Q(t)$  at any chosen time within our data record. A corresponding integration of the right-hand side, assuming we know the law relating the variation of resistivity and density with heat content, would then relate the measured heat input to the resulting heat content per unit mass of the liquid core.

Unfortunately,  $\rho(q)$  has not been measured at sufficiently high temperatures for most metals. A further complication is that the model assumed thus far is an average one, in the sense that both  $\rho$  and  $d$  apply here to the assumed uniform cylinder employed to represent the actual conducting path. In order to proceed, we use an extrapolation of the values of  $\rho d$  measured at the lower  $q$  values before the vaporization becomes important. For those  $q$  values between melt,  $q_m$ , and the onset of vaporization,  $q(\text{vap})$ , we note that  $m_2 = m_3$  and  $r_2(t) = r_1(t)$ . Using the latter relations in Eqns. (17) and (18) gives

$$R_2/R_0 = \frac{\rho(t)}{\rho_0} \frac{d(t)}{d_0} \quad \text{for } q \text{ between } q_m \text{ and } q(\text{vap}). \quad \text{Plots of } R_2/R_0 \text{ vs. } q$$

in this energy range indicate a linear relation between the product  $\rho d$  and  $q$ . We assume that this linear relation continues to hold for  $q > q(\text{vap})$ ; this assumption enables us to integrate the right-hand side of Eq. (19) with respect to  $q(t)$ . The resulting integral relation, evaluated numerically, correlates the measured input heat energy,  $Q(t) - Q_0$ , with the heat content per unit mass,  $q(t)$ , of the liquid core.

Using Eqns. (17) and (18) we then have

$$m_2/m_3 = (\rho(t)/\rho_0) (d(t)/d_0) (R_0/R_2(t)) \quad (20)$$

for the range  $q(t) > q(\text{vap})$ . Since the right-hand side is now known as a function of time, numerical differentiation with respect to  $t$  can be done for use in Eq. (16). If one moreover knows how  $r_1[q(t)]$  varies with  $q(t)$ , then  $c_r$  is obtained as a function of  $q$ . By hypothesis,  $r_1(t)/r_0$  is  $\{d_0/d(t)\}^{\frac{1}{2}}$ , so one needs  $d[q(t)]$  as a function of  $q$ . Since the density,  $d(q)$ , is expected to decrease with  $q$ , it follows that  $r_1(q)$  should increase with  $q$ . If one uses the modified van der Waals theory described previously, assumes the state of the liquid core to be that of the saturated liquid, and takes the reference conditions to correspond to those of the liquid at melt, one finds  $d(q)/d_m$  decreases slowly from the value unity until  $q$  values near critical are approached.

If we define

$$c_{r_0}(q) = -r_s \frac{d(m_2/m_3)^{\frac{1}{2}}}{dt} \quad (21)$$

where  $r_s$  is the original radius of the solid wire, we have from Eq. (16)

$$c_r(q) = F(q) c_{r_0}(q) , \quad (22)$$

where

$$F(q) = \left(\frac{r_0}{r_s}\right) \left(\frac{r_1(q)}{r_0}\right) . \quad (23)$$

The quantity  $c_{T_0}(q)$  is obtained directly from the electrical data using the model just described. On the other hand,  $F(q)$  depends on the thermal expansion of the liquid, and cannot be obtained from our present data. Estimates of  $F(q)$  indicate it may be replaced by a constant a little larger than unity for temperatures less than .9 critical.  $F(q)$  will be described more completely below. For the present, we show experimental values of  $c_{T_0}$  versus  $q$ .

#### Experimental Conditions

Using the above procedure, we have obtained experimental values of  $c_{T_0}$  versus  $q$  from tests on copper, lead, aluminum, gold silver, and mercury wires. The copper data have been reported previously,<sup>2</sup> although not in the scaled form given here. We first mention briefly the experimental conditions and give tables of pertinent quantities.

A capacitor of 31.5  $\mu$ F was used for all tests except those on copper, and the circuit ringing frequency was 43 kc/sec. Voltage and current traces were photographed on a type 555, double-beam Tektronix oscilloscope. From measurements of these traces we

obtain  $V_R(t)$  and  $I(t)$ ; numerical integration gives  $\Delta Q(t) = \int_0^t V_R I d\tau$ ,

and we have  $R_2(t) = V_R/I$ . We list in Table I the conditions for all wires except copper; copper test conditions are given in Ref. 2. The explosions occurred in air at atmospheric pressure, and the wires were maintained at room temperature before current switch-on, except for the frozen mercury wires; they were kept at dry ice-acetone temperatures.

From the measurements, the scaled functions  $S_2(t) = R_2 \pi r_3^2/l$  and  $U(t) = \Delta Q(t)/m_3$  were plotted as ordinate and abscissa, respectively, for each metal; here  $r_3$  and  $m_3$  are the initial radius and mass of the wires. For a given metal we find that the  $S_2$  vs.  $U$  plots for wires of different radii and initial capacitor voltage coincide with each other until a fixed value of  $U$  is exceeded. For  $U > U_v$ , the plots diverge from each other, according to initial wire diameter and capacitor voltage.<sup>2\*</sup>

For  $U$  between a typical low value,  $U_m$ , and the higher value  $U_v$ , the experimental functions  $S_2$  vs.  $U$  can be approximated by a straight line segment for each metal. On this segment,  $S_2 = S_0\{1 + \beta(U - U_0)\}$ ; then the ratio  $S_2/S_0 = R_2/R_0$  as defined by Eq. (17), and we take our reference conditions  $(S_0, V_0)$  at the largest value of  $U = U_v$  where the experimental curves depart significantly from linearity. Table II gives the experimental quantities typifying these straight line segments for the different metals. The last column,  $\Delta q_1$ , is the computed heat content per unit mass of metal prior to electrical heat addition.

---

\* The notation of Ref. 2 is slightly different from that used here. A factor  $\pi$  was inadvertently omitted from the ordinate of Fig. 4 reproduced there.

Table I. Test Conditions

| <u>Metal</u> | <u>Initial Wire Diameter</u> |             | <u>Length (cm)</u> | <u>Initial Capacitor Voltage (kV)</u> | <u>No. of Tests</u> |
|--------------|------------------------------|-------------|--------------------|---------------------------------------|---------------------|
|              | <u>(mils)</u>                | <u>(cm)</u> |                    |                                       |                     |
| Lead         | 5.1                          | .0130       | 1.1                | 1.2                                   | 1                   |
| Lead         | 10                           | .0254       | 1.0                | 1.0                                   | 1                   |
| Lead         | 10                           | .0254       | 1.0                | 2.0                                   | 1                   |
| Lead         | 10                           | .0254       | 1.0                | 3.0                                   | 1                   |
| Aluminum     | 5.6                          | .0142       | 1.1                | 2.0                                   | 1                   |
| Aluminum     | 10                           | .0254       | 1.1                | 3.0                                   | 2                   |
| Gold         | 10                           | .0254       | 2.0                | 3.0                                   | 2                   |
| Silver       | 10                           | .0254       | 2.0                | 3.0                                   | 1                   |
| Mercury      | 20                           | .0508       | 2.0                | 2.5                                   | 1                   |
| Mercury      | 20                           | .0508       | 2.0                | 3.0                                   | 1                   |

Table II. Resistive and Heat Input Measurements

First column gives tabulated values of liquid resistivity at melt (Ref. 7). Last column gives heat content prior to test, estimated from tabulated specific heats

| <u>Metal</u> | $\rho_m$<br>( $\mu\Omega$ -cm) | $S_m$<br>( $\mu\Omega$ -cm) | $U_m$<br>( $\frac{kJ}{gm}$ ) | $\frac{dS}{dU}$ (linear)<br>( $\frac{\mu\Omega$ -cm)<br>( $\frac{kJ}{gm}$ ) | $S_o$<br>( $\mu\Omega$ -cm) | $U_o$<br>( $\frac{kJ}{gm}$ ) | $\Delta q_1$<br>( $\frac{kJ}{gm}$ ) |
|--------------|--------------------------------|-----------------------------|------------------------------|---|-----------------------------|------------------------------|-------------------------------------|
| Copper       | 21.1                           | 29                          | 1.10                         | 8.40  | 40.5                        | 2.4                          | .083                                |
| Lead         | 95                             | 102                         | .085                         | 144   | 146                         | .39                          | .035                                |
| Aluminum     | 24.2                           | 26                          | 1.4                          | 5.1   | 48                          | 5.7                          | .20                                 |
| Gold         | 31.2                           | 35                          | .35                          | 66  | 60                          | .72                          | .031                                |
| Silver       | 17.2                           | 19                          | .75                          | 22.6  | 28                          | 1.14                         | .063                                |
| Mercury      | 91                             | 108                         | .045                         | 700   | 125                         | .07                          | .030                                |

The value  $S_M = S_g(U_M)$  should be comparable with the resistivity of the liquid metal at melt,  $\rho_M$ . Previously tabulated values of  $\rho_M$  are given in the first column.<sup>7</sup> Assuming the wire length constant, one expects  $\rho_M = S_M(d_s/d_M)$  where  $d_s/d_M$  is the ratio of solid density to the liquid density at melt, a factor about 7 to 12 percent greater than unity for these metals. Thus, one expects  $\rho_M$  several per cent larger than our measured  $S_M$ , whereas we find the converse in these experiments.

Extra care was taken with the frozen mercury wires,<sup>\*</sup> both to prevent premature melting and to contain the metal vapor. A special, electrode cell was constructed and cooled to the dry ice-acetone temperature. The wire was attached to the electrodes and the electrodes were enclosed by a lucite cylinder of two inches in diameter, sealed with O rings. This cell was placed in the circuit and energized within seconds after removal from the cold box. Even with these precautions, erratic electrical behavior was noted on a number of trials with the frozen mercury wires. In at least one case the wire melted before the current pulse was applied. In another, examination of unused portions of the wire disclosed remnants of the glass capillary not completely dissolved away. Only two of the mercury tests were judged worthy of data reduction.

---

*\*We are particularly indebted to A.V. Grosse, J. Cahill and Mrs. L. Streng of the Research Institute of Temple University for supplying the frozen mercury wires. The wires tested thus far were made by freezing mercury in capillary tubes and dissolving the capillary in acid.*

### Experimental Wave Speeds

We show in Fig. 4 the experimental results in deducing  $c_{T_0}$  and  $q$  from the data. The  $q$  values contain the computed heat content of the solid metal just before the test, as given by  $\Delta q_1$  in Table II. Data points connected by a given line were obtained from a single explosion.

We attempt to correlate the data from the different metals by dividing  $c_{T_0}$  by  $\{\hat{R}T_c\}^{\frac{1}{2}}$  and  $q$  by  $\hat{R}T_c$  to give  $\bar{c}_{T_0}$  and  $\bar{q}$ ; the resulting plot is shown in Fig. 5. Only the bounds of the data are indicated for copper, lead and aluminum. The critical temperatures,  $T_c$ , used here are those estimated by A. V. Grosse and his associates.<sup>8,9,10</sup> These and other constants are given in Table III.

The experimental curves  $\bar{c}_{T_0}$  for the different metals (excepting mercury) are seen to coincide only at the lower values of  $\bar{q}$  where the experimental wave speeds begin to be detectable. This scaled heat content of wave onset is about  $2.1 \pm 0.2$ . Taking this fact as an experimental test of the critical temperatures used for the scaling, then the values used for  $T_c$  appear to be satisfactory within the  $\pm 10$  percent data scatter.

At heat contents higher than that of wave onset, the scaled curves for the different metals depart from each other. In particular, those for the monetary metals, copper and silver, bend to the right and go to scaled heat contents considerably higher than the other metals. We note  $c_{T_0}$  should be multiplied by the factor  $F(q/\hat{R}T_c)$  defined in Eq. (23)

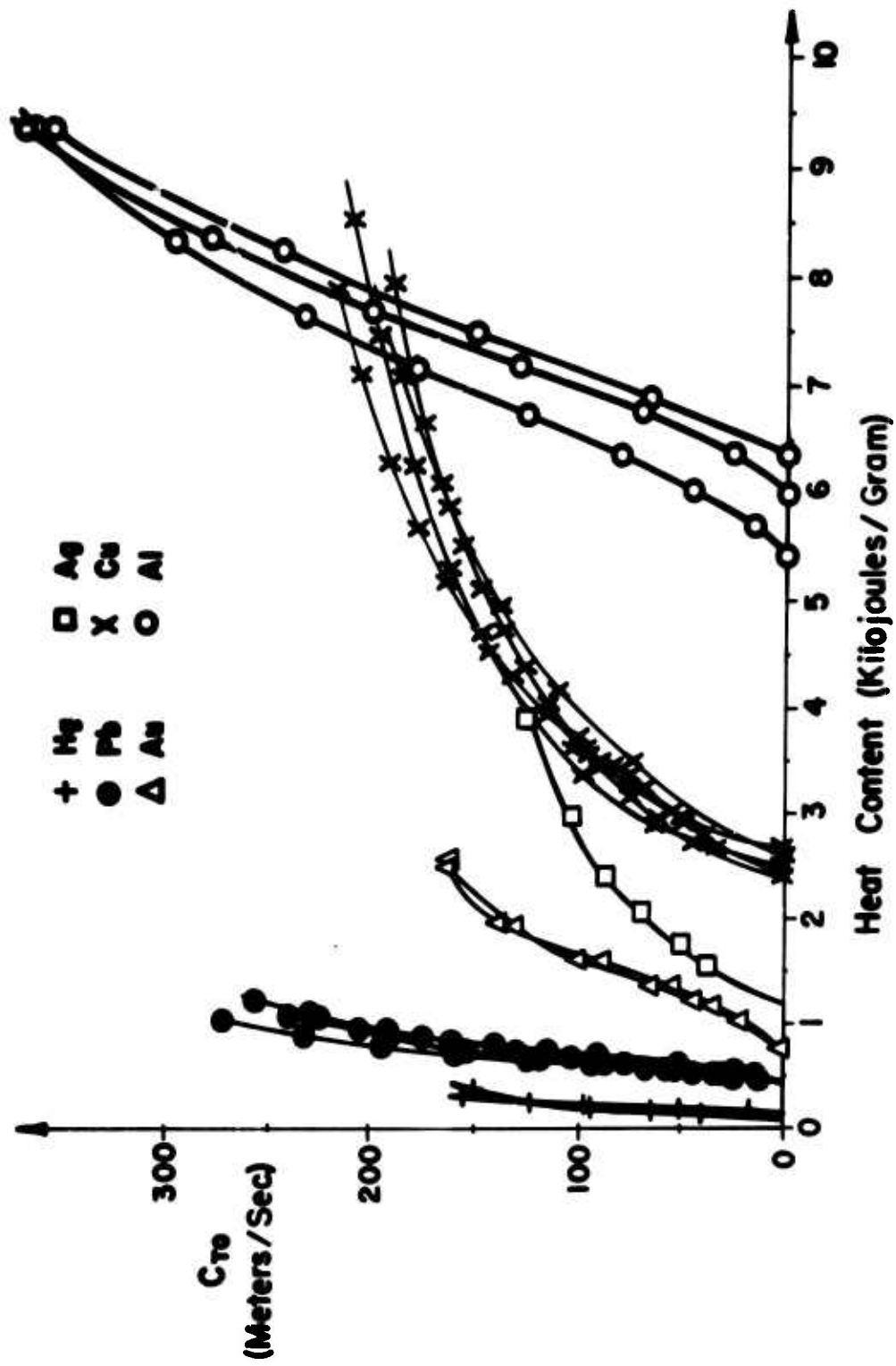


Figure 4. Experimental wave speeds. Thermal expansion of the core has been neglected

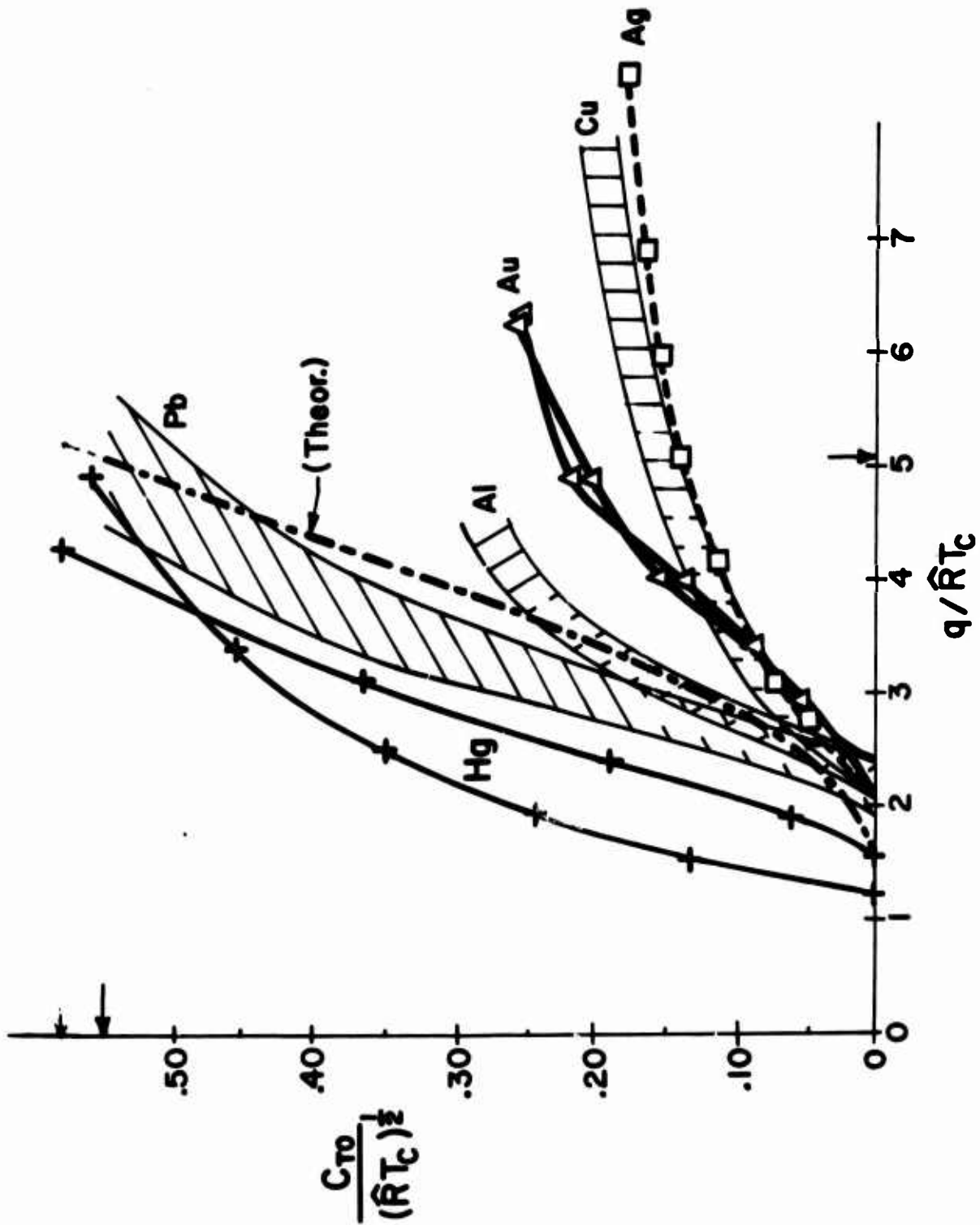


Figure 5. Scaled wave speeds. Theoretical curve is vaporizing sound speed [center curve of Figure 3, adjusted 0.1 unit right for  $q(T_M)$ ]. Arrows show critical point limits for theoretical curve

Table III. Scaling Constants

First column gives estimated critical temperatures  
(Refs. 8, 9, 10)

| <u>Metal</u> | $T_c$<br>(°K) | T(melt)<br>(°K) | M<br>(gm/mol) | $\hat{RT}_c$<br>(kJ/gm) | $(\hat{RT}_c)^{\frac{1}{2}}$<br>(m/sec) |
|--------------|---------------|-----------------|---------------|-------------------------|---|
| Copper       | 8500          | 1356            | 63.5          | 1.088                   | 1043                                    |
| Lead         | 5400          | 601             | 207.2         | .217                    | 465                                     |
| Aluminum     | 8650          | 933             | 27.0          | 2.67                    | 1633                                    |
| Gold         | 9500          | 1336            | 197.2         | .401                    | 630                                     |
| Silver       | 7460          | 1234            | 107.9         | .575                    | 758                                     |
| Mercury      | 1733          | 234             | 200.6         | .0718                   | 268                                     |

to obtain the scaled local velocity of the nonconducting wave front,  $\bar{c}_1$ . If this factor were the same for the different metals, its use would not improve the correlation of  $\bar{c}_1$  over that of the  $\bar{c}_{10}$  quantities. It is possible to compute a theoretical  $F(q/\hat{RT}_c)$  curve using the modified van der Waals model described above. Aside from insignificant differences caused by assuming different values of specific heat of the liquid,  $C_v/\hat{R}$ , this theoretical curve is identical for all the metals. Moreover, the theoretical curve is not defined for  $\bar{q}$  values larger than that corresponding to the critical point. We show this curve in Fig. 6 for the example where  $C_v(\text{liq}) = (5/2)\hat{R}$ , and  $C_v(\text{vap}) = (3/2)\hat{R}$ . For this same example, we also show on Fig. 5 the scaled theoretical vaporizing sound speed,  $\bar{c}_w = c_w/(\hat{RT}_c)^{1/2}$ . This curve terminates at  $\bar{q} \approx 5$ . We expect the speed of the wave front,  $c_1$ , to be closely related to the vaporizing sound speed,  $c_w$ , along the saturated liquid line of the metal. Note that the experimental data for copper and silver greatly exceed the limiting heat content of the theoretical curve. The simplifying assumption of a linear extrapolation of  $\rho d$  to the higher heat energies may be questionable for these metals.

None of the wave speed data shown here was obtained from electrical data at times larger than that corresponding to a 10 percent descent of the voltage past its peak value. Two reasons for choice of this limiting time are: (a) In those tests where initial capacitor voltages are "well matched"<sup>6</sup> to the wire, the very rapid decrease of

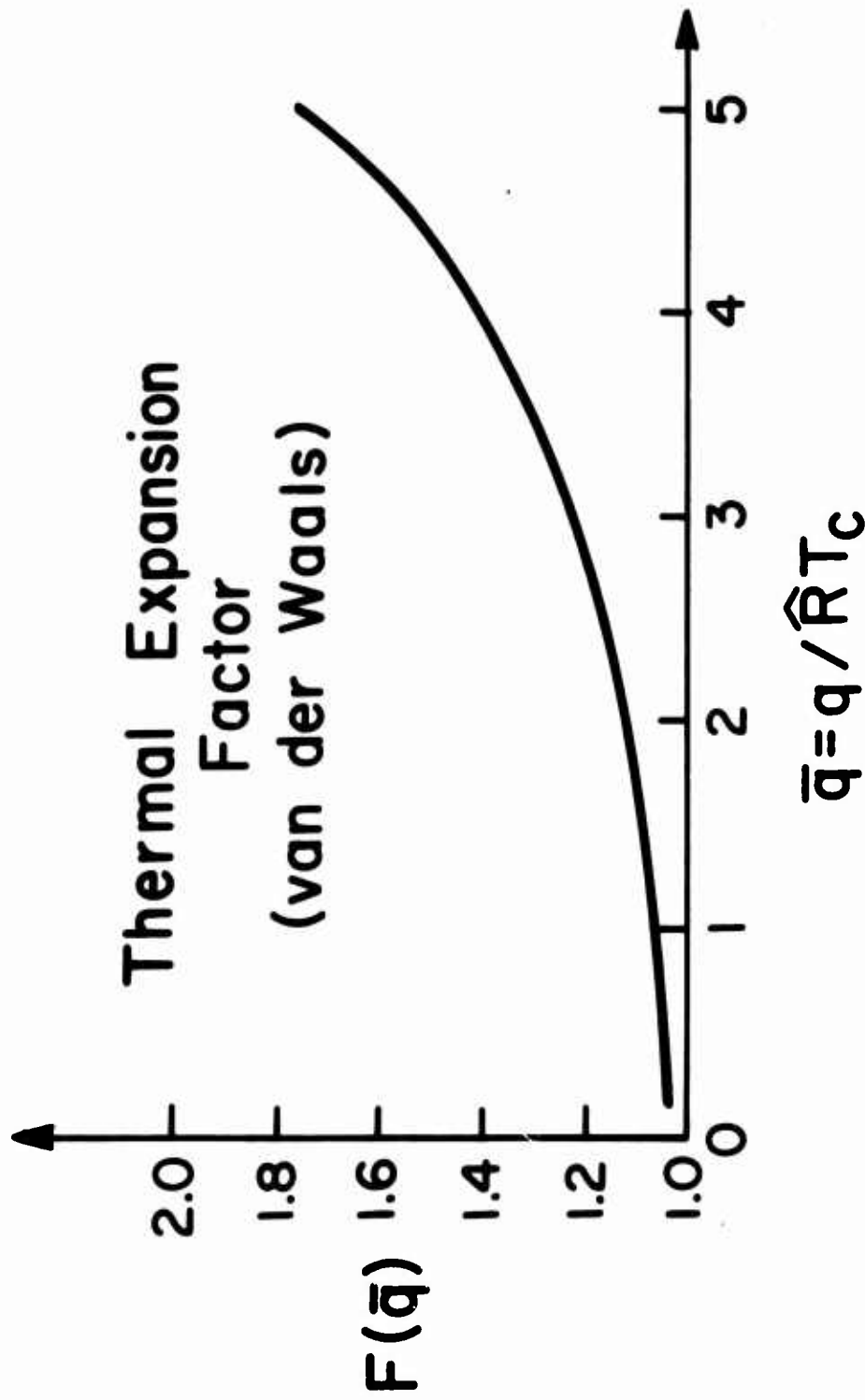


Figure 6. Factor accounting for thermal expansion of liquid. A modified van der Waals model  $[C_v(\text{liq}) = (5/2)\hat{R}, C_v(\text{vap}) = (3/2)\hat{R}]$  is used

both voltage and current with time after the voltage peak makes the resistance measurements inaccurate; and (b) In those instances where the capacitor voltage is not "well matched," the measured resistance reaches a maximum and then decreases, suggesting the occurrence of arc breakdown. In a given test, when the curvature of the  $R_2$  vs.  $U$  curve changes from concave upward, no further data from that test are used.

#### DISCUSSION

The present experiments are somewhat ambiguous on the question of the vaporization wave hypothesis. If there were no agreement between the experimental findings and the theoretical implications of the wave speed and thermodynamic models, one could reject the hypothesis as incorrect. On the other hand the agreement between experimental and theoretical wave speeds is sufficiently good so that the wave speed model continues to survive as a partial explanation of the expansion process.

The assumption of an incoming, cylindrical wave front separating the conducting core from the nonconducting wet vapor enables one to deduce front velocities which are comparable with the vaporizing sound speed of the saturated liquid. No other signal speed, either suggested or measured from thermodynamic data, is of the same order of magnitude as the vaporizing sound speed.

When different metals are considered, the use of a similarity law suggested by the theory permits correlation of the lower temperature wave speeds within a reasonably narrow band. This convenient scaling which harmonizes the data for the various metals, permits detailed comparisons which reveal significant differences between them. For example, the effects of adjusting critical temperatures to improve the correlation can easily be seen.

The method of data analysis identifies the radius-time locus of that front which by hypothesis abruptly separates the finite conductivity of the intact liquid core from zero conductivity vapor. Such a locus probably does not exist physically; yet it is in a sense analogous to the boundary layer displacement thickness of a viscous fluid flow, and plays a similarly useful role in treating a complicated problem. From physical grounds, one can maintain that the electrical conductivity, on the average, varies as a continuous function of radius, decreasing from that of the liquid metal core at the radius of the leading edge of the vaporizing expansion wave, to zero at some larger radius. If this argument is admitted, then the average radius of the front which abruptly separates finite from zero conductivity must be larger than that of the leading edge of the vaporizing expansion wave. The reasoning proceeds as follows: The transition region of conductivity fans out with time, as all finite expansion waves do, and the abrupt change in conductivity must fall relatively further behind the head of the expansion wave; hence, the speed of this assumed front would be lower than that of the

vaporizing sound speed in the molten metal. The experimental values for the noble metals appear to lie below the theoretical curve even after estimated corrections for dilatation; i.e., multiplication by  $F(\bar{q})$ , are applied.

The good agreement of wave onset for the different metals at the lower specific energies probably reflects both the fact that the assumed linear behavior of  $\rho d$  with  $q$  cannot be greatly in error here, and also the likelihood that the early trajectories of both the average conductivity wave front and the vaporization wave front are closely coincidental. The divergence of the curves for the different metals at higher specific energies, and the fact that finite wave front velocities for copper and silver are obtained at energies greatly in excess of those expected to drive the metal past critical temperature, cannot be explained merely by revising the linear extrapolation of  $\rho d$ .

The abundant data for copper<sup>2\*</sup> exhibit large and increasing resistances at specific energies sufficiently high to heat the original mass of copper well beyond critical temperatures. This fact is independent of any assumption about the behavior of the product  $\rho d$  for the

---

\*See Fig. 4 of this reference where resistance data for several wires are plotted versus specific energy obtained by dividing the total deposited energy at a given time by the initial wire mass.

saturated liquid. One is forced to conclude that the supercritical copper must have a finite resistivity both in the core and in the denser parts of the expanding flow. Thus, it follows that the electrical resistivity of the metal vapor is an important parameter in fixing the position of the wave front which shuts off conduction. With this added parameter whose effects cannot yet be accounted for, one should not expect perfect correlation of the conduction-front, wave speeds for the different metals when using a scaling law based on mechanical and thermodynamical arguments alone. The present scaling law should apply to the electrical wave fronts only when the vaporization and electrical conduction waves are nearly coincident, as they are expected to be at wave onset.

The physical properties of supercritical materials at high densities are not well known, but there are some theoretical reasons<sup>3,11</sup> for thinking that electrical conductivity may persist or even be enhanced in materials at temperatures above critical and at normal liquid densities. According to Rouse's calculations made with a modified Saha equation, copper at normal densities and temperatures near 1 eV will have up to 15 percent concentration of the first ion present on account of pressure ionization. Presumably the free electrons will participate in conduction and Ohmic heating processes as usual. Thus, arguments based on the presumed zero conductivity of condensing materials above the critical temperature can be seriously in error. If this is the case, the

indicated high temperatures may be real and the temperature multiplying capabilities of the exploding wire experiment are realized in practice. Since the argument of an earlier paragraph shows that the most conservative method of calculating specific energies for copper leads to the conclusion that supercritical temperatures ( $T_c \sim 8500^\circ\text{K}$  for Cu) are indeed attained, the conclusion seems inescapable that some process capable of increasing the number of current carriers, e.g., pressure ionization of the neutral atoms, is an important factor at the higher temperatures and densities encountered in the wire cores.

A further anomaly in the thermal behavior of the metals studied should be noted. The measured input heat energy to the wires always appears to be larger than expected. For example, the experimental heat content of the liquid at melt is always larger than that computed by using tabulated specific heats and heats of fusion. For the listed metals in Table II, these excesses are respectively, 55, 20, 30, 80, 100 and 90 percent. The point corresponding to the liquid at melt is taken where the  $S_2$  vs.  $U$  curves first show an abrupt decrease of slope to the linear portion; this point also corresponds to the first abrupt slope decrease easily visible on the voltage-time curve. The slope of the linear portion of the  $S_2, U$  curve can be related to tabulated values of the temperature coefficient of liquid resistivity. Even after accounting for the expected volume change, and using the best estimated values for liquid specific heat, the experimental slope is smaller than expected. Conversely, for a given liquid resistivity, the corresponding

heat content from the present data is much higher than that obtained using handbook values for the temperature coefficient of liquid resistivity.

The presence of the striations at an early stage, as discovered by Fansler and Shear,<sup>4</sup> at first appears to be a strong argument against the existence of a vaporization wave phenomenon. The striations do in fact rule out the possibility that the vaporization wave proceeds uniformly into the material on a front with cylindrical symmetry about the wire axis. Rather one must argue that as vaporization begins at temperatures far below critical and with specific energies too small to produce complete vaporization, the striations may be the physical evidence of the random, statistical way in which vaporization takes place at favored surface sites, during passage of the wave. The shape and number of striations may be indications of the manner in which small regions are cooled by local, thermal transport processes to support the vaporization of adjacent regions. If so, this new hypothesis would force a reconsideration of our primitive ideas of the symmetry of the process of vaporization, but not necessarily a revision of its fundamental basis. Clearly, such a view of the striation problem provides an alternative, or a supplement, to theories based on assumption of the prior existence of elastic or plastic waves, buckling phenomena and the like.

## SUMMARY

The energy dependent expansion of a cylinder of superheated liquid is offered as an idealized, physical model of flow phenomena occurring in exploding wire events. Magnified streak shadowgraphs of Cu wires show complex radial motions accompanying two major stages, viz: (1) a linear boundary expansion during which a vapor veil proceeds ahead of a denser expanding core and, (2) a parabolic boundary expansion characterized by violent acceleration of the inner core as a result of sudden energy addition. Correlated electrical data show that the main deposit of electrical energy occurs near the end of the linear expansion during which the vaporization wave is presumed to initiate the expansion.

Vaporization wave speeds have been obtained from experiments on wires of Al, Pb, Ag, Cu and Au and from the first, preliminary experiments on solid Hg wires. The wave-speed curves for these metals show similar behavior although the initial specific energies differ by a factor up to  $10^2$ . A thermodynamic model of the expansion is obtained by assuming a modified van der Waals equation of state together with a state path lying on the liquidus line in the  $p - \hat{v}$  plane. Values of the adiabatic sound speed calculated from the thermodynamic model and representing expansions from the liquidus line into the two-phase region, agree well with the initial portions of the experimental wave speed curves. When speed is scaled by  $(RT_c)^{\frac{1}{2}}$  and specific energy by  $RT_c$ , a plot of corresponding states is obtained wherein for all the metals the experimental data initially overlap the theoretical curve but

deviate in different ways at larger values of the scaled variables.

Discussion of these deviations shows that to some extent they can be attributed to the approximations inherent in the fluid dynamic and thermodynamic models, and to assumptions made necessary by the lack of electrical and thermal data for the elements.

#### ACKNOWLEDGMENTS

The authors are grateful to Mr. D. D. Shear and Mr. T. Long for performing the experiments, to Mr. H. S. Burden who assisted with the data measurement and reduction, and to Mr. D. C. Mylin who made many of the numerical computations.

#### REFERENCES

1. F. D. Bennett, *Phys. Fluids* 8, 1425 (1965).
2. F. D. Bennett, G. D. Kahl and E. H. Wedemeyer in Exploding Wires, Vol. 3, edited by W. G. Chace and H. K. Moore (Plenum Press, Inc., New York, 1964), p. 65.
3. F. D. Bennett, *Phys. Fluids* 8, 1106 (1965).
4. K. S. Fansler and D. D. Shear, Exploding Wires, Vol. 4, edited by W. G. Chace and H. K. Moore (Plenum Press, Inc., New York, 1968).
5. G. D. Kahl, *Phys. Rev.* 155, 78 (1967).
6. F. D. Bennett, H. S. Burden and D. D. Shear, *Phys. Fluids* 5, 102 (1962).
7. N. E. Cusack, Rep. Prog. in Physics, XXVI, (The Institute of Physics and the Physical Society, Stonebridge Press, Bristol, England, 1963) p. 361.
8. A. V. Grosse, *J. Inorg. Nucl. Chem.* 22, 23 (1961).
9. J. A. Cahill and A. D. Kirshenbaum, *J. Phys. Chem.* 66, 1050 (1962).
10. A. V. Grosse, *Rev. Hautes Temper. et Refract.*, t. 3 1966, N° 2, pp. 115-146.
11. C. A. Rouse, *Astrophys. J.* 139, 339 (1964).

DOCUMENT CONTROL DATA - R & D

(Security classification of title, body of abstract and indexing annotation must be entered when the overall report is classified)

|   |  |  |                       |
|---|--|--|-----------------------|
| 1. ORIGINATING ACTIVITY (Corporate author)<br>U.S. Army Ballistic Research Laboratories<br>Aberdeen Proving Ground, Maryland  |  | 2a. REPORT SECURITY CLASSIFICATION<br>Unclassified                                 |                       |
|   |  | 2b. GROUP  |                       |
| 3. REPORT TITLE<br>VAPORIZATION WAVES IN METALS   |  |  |                       |
| 4. DESCRIPTIVE NOTES (Type of report and inclusive dates)   |  |  |                       |
| 5. AUTHOR(S) (First name, middle initial, last name)<br>Frederick D. Bennett and George D. Kanl   |  |  |                       |
| 6. REPORT DATE<br>November 1967   |  | 7a. TOTAL NO. OF PAGES<br>55   | 7b. NO. OF REFS<br>11 |
| 8a. CONTRACT OR GRANT NO.   |  | 8b. ORIGINATOR'S REPORT NUMBER(S)<br>Report No. 1383                               |                       |
| b. PROJECT NO. RDT&E 1T014501A33D   |  |  |                       |
| c.  |  | 8c. OTHER REPORT NO(S) (Any other numbers that may be assigned this report)        |                       |
| d.  |  |  |                       |
| 10. DISTRIBUTION STATEMENT<br>This document has been approved for public release and sale; its distribution is unlimited.   |  |  |                       |
| 11. SUPPLEMENTARY NOTES   |  | 12. SPONSORING MILITARY ACTIVITY<br>U.S. Army Materiel Command<br>Washington, D.C. |                       |
| 13. ABSTRACT<br>The vaporization wave hypothesis is discussed and its merits and defects are examined. The vaporizing model is visualized on thermodynamic grounds as carrying the liquid metal through a continuous succession of states either on or near the liquidus line in the two-phase region. On this line the adiabatic sound speed for wet vapor will limit the rate of propagation of the vaporization front into the liquid. Experimental data for wire explosions of Al, Ag, Cu, Au, Pb and Hg (frozen) are analyzed for wave speeds. While the influence of thermal expansions of the liquid can be accounted for theoretically, insufficient thermal data are available for the metals to permit correction of the wave speeds for this effect. The experimentally derived wave speeds are compared with theoretical values of the adiabatic sound speed in the wet vapor obtained from a modified, van der Waals equation of state. At low velocities the agreement is satisfactory but higher values deviate considerably from theory. Possible causes of the deviations are discussed. These include the crudity of the fluid dynamic model, neglect of thermal expansion, lack of information about the relationship between density and electrical conductivity and the approximation imposed by the van der Waals equation. |  |  |                       |

Unclassified

Security Classification

| 14. KEY WORDS  | LINK A |    | LINK B |    | LINK C |    |
|--|--------|----|--------|----|--------|----|
|  | ROLE   | WT | ROLE   | WT | ROLE   | WT |
| Exploding Wires<br>Equation of State<br>Thermodynamics<br>Thermodynamics of Metals<br>Vaporization Waves<br>High Temperature Physics |        |    |        |    |        |    |

Unclassified  
Security Classification